Structure and magnetism of collapsed lanthanide elements

On the Structures and Magnetism of Collapsed Lanthanide Elements

M.I. McMahon,[1] S. Finnegan,[1] R.J. Husband,[1] K.A. Munro,[1] E. Plekhanov,[2]
N. Bonini,[2] C. Weber,[2] M. Hanfland,[3] U. Schwarz,[4] and S.G Macleod[5]

[1]*SUPA, School of Physics and Astronomy, and Centre for Science at Extreme Conditions, The University of Edinburgh, Mayfield Road, Edinburgh, EH9 3JZ, UK.*
[2]*King's College London, Physics Department, The Strand, London WC2R 2LS, United Kingdom*
[3]*European Synchrotron Radiation Facility, 38043 Grenoble, France*
[4]*Max Planck Institut fr Chemische Physik fester Stoffe, Nthnitzer Straße 40, D-01187 Dresden, Germany*
[5]*Atomic Weapons Establishment, Aldermaston, Reading, RG7 4PR, United Kingdom*

(Dated: June 26, 2019)

Using synchrotron X-ray diffraction, we show that the long-accepted monoclinic structure of the "collapsed" high-pressure phases reported in seven lanthanide elements (Nd, Tb, Gd, Dy, Ho, Er and (probably) Tm) is incorrect. In Tb, Gd, Dy, Ho, Er and Tm we show that the collapsed phases have a 16-atom orthorhombic structure ($oF16$) not previously seen in the elements, while in Nd we show that it has an 8-atom orthorhombic structure ($oF8$) previously reported in several actinide elements. $oF16$ and $oF8$ are members of a new family of layered elemental structures, the discovery of which reveals that the high-pressure structural systematics of the lanthanides, actinides and group 3 elements (Sc and Y) are much more related that previously imagined. Electronic structure calculations of Tb, combined with quantum many body corrections, confirm the experimental observation, and calculate that the collapsed orthorhombic phase is a ferromagnet, nearly degenerate with an anti-ferromagnetic state between 60 and 80 GPa. We find that the magnetic properties of Tb survive to the highest pressures obtained in our experiments (110 GPa). Further calculations of the collapsed phases of Gd and Dy, again using the correct crystal structure, show the former to be a type-A antiferromagnet, while the latter is ferromagnetic.

PACS numbers: 61.50.Ks,62.50.+p

I. INTRODUCTION

The lanthanide (Ce to Lu) and actinide (Th to Lr) series of metals are characterised by the monotonic increase in the number of their $4f$ and $5f$ electrons, respectively. As electron interactions can be readily modified by changing interatomic distances, studies of the lanthanide and actinide elements under compression have been critical in developing an understanding of f-electron behaviour at high densities[1–6]. The f electrons in both series of elements are usually classified as being either localised, and characterised by tightly-bound shells or narrow bands of highly correlated electrons near the Fermi level, or itinerant and able to participate in the metallic bonding[5]. In the regular trivalent lanthanides (Ce to Lu, excluding Eu and Yb) the $4f$ electrons are localised at ambient conditions, and, on compression, an increase in d-band occupancy resulting from s-d electron transfer gives rise to a common phase transition sequence between structures comprising different stackings of close-packed layers: hcp (space group $P6_3/mmc$ and $hP2$ in Pearson notation) $\rightarrow$ Sm-type ($R\bar{3}m$ and $hR3$) $\rightarrow$ double-hcp ($P6_3/mmc$ and $hP4$) $\rightarrow$ fcc ($Fm\bar{3}m$ and $cF4$) $\rightarrow$ distorted-fcc ($R\bar{3}m$ and $hR24$) ([5,6], and references therein). While there are no measurable volume changes between any of these different phases, neither do any of them have group-subgroup relationships. Indeed, Porsch and Holzapfel studied the symmetry changes at the $cF4 \rightarrow hR24$ transition in detail, and showed that it must be first order[7].

When compressed further, the $hR24$ phases transform to lower-symmetry "collapsed" phases, often via a sudden decrease in atomic volume ([6], and references therein). Similar behaviour is observed in the trans-Pu "heavy" actinide elements (Am[8], Cm[9] and Cf[10]) on compression, each of which transforms via volume discontinuities to complex structural forms seen in the lighter actinides (Th - Pu). Volume discontinuities and the appearance of low-symmetry structures are commonly associated with the pressure-induced delocalisation of the $4f/5f$ electrons and their subsequent participation in bonding. However, recent X-ray spectroscopy measurements on Tb to extreme pressure reveal that neither a valence change nor $4f$ delocalisation occur at the volume collapse pressure of 53 GPa[11]. Rather, the collapsed phases of both Tb and neighbouring Dy exhibit anomalously-high magnetic ordering temperatures suggestive of an unconventional magnetic state[12,13]. Understanding the mechanism(s) responsible for these high ordering temperatures might enable their reproduction in a suitable compound at ambient pressure, leading to the synthesis of superior permanent magnet materials.

The collapsed phases in the regular lanthanides are most commonly reported to have a 4-atom monoclinic structure with spacegroup $C2/m$ ($mC4$ in the Pearson notation) first observed in Ce 40 years ago[16]. Since then, the collapsed phases of Nd, Sm, Gd, Tb, Dy, Ho, Er and Tm have all been reported to have the same $mC4$ structure ([6], and references therein), such that it is now *the*

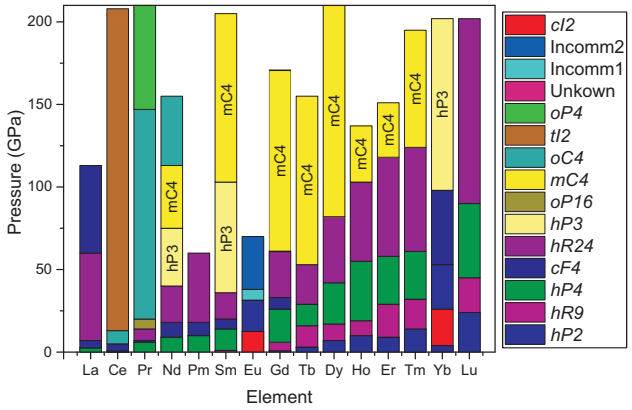

FIG. 1: The different phases reported in the lanthanide elements up to 210 GPa at ambient temperature. Transition pressures are taken from Ref[6,14,15] and references therein. The collapsed $mC4$ and $hP3$ phases are highlighted in full and pale yellow, respectively, and are labelled. Of the low-symmetry phases, only the $oC4$ and $tI2$ phases are also seen in the actinides.

key structure in the lanthanide elements at high densities (see Figure 1). In Nd and Sm, the $mC4$ phase is obtained via an intermediate rhombohedral $hP3$ phase (spacegroup $P3_121$, but see later) seen only in these two elements[17,18] and Yb[19]. And in Ce, Pr and Nd, a collapsed phase with the orthorhombic structure found in uranium at ambient conditions (space group $Cmcm$ and Pearson notation $oC4$) is also found[20–22]; somewhat surprisingly, this, and the tetragonal $tI2$ phase seen in Ce and Th[23,24], are the only non-cubic crystal structures that the lanthanides and actinides have in common on compression.

There is thus a consensus, constructed over decades, as to the structural behaviour of the lanthanides on compression, as illustrated in Figure 1, and the phases which are common to both lanthanides and actinides. However, while the similarity of many of the published diffraction patterns from the collapsed phases of the lanthanides suggests they do share a common structure, the widely-reported $mC4$ monoclinic structure provides an inadequate fit to many, if not all of them – as detailed in the Supplementary Material[25].

Using high-quality synchrotron X-ray diffraction data, we have determined the correct structure of the collapsed phase of Tb as orthorhombic, with spacegroup $Fddd$, and 16 atoms per unit cell ($oF16$). Furthermore, we show that the same $oF16$ structure better fits the published diffraction data from the collapsed phases of Dy, Ho, Er and Tm, as well as data we have collected from the collapsed phase of Gd. The $oF16$ structure comprises a stacking of eight quasi-close-packed layers, and is isosymmetric with the structure found previously in Pu, Cf, Am and Cm - although with a 4-layer stacking sequence in those cases ($oF8$). We show that the $hP3$ structure of Nd, Sm and Yb comprises a similar 3-layer stacking sequence of the same quasi-close packed layers, and hence that the $hP3$, $oF8$ and $oF16$ structures form a new family of layered elemental crystal structures, differing only in the stacking sequence of their atomic layers.

The correct determination of the structures of the collapsed phases of Nd, Gd, Tb, Dy, Ho, Er and Tm greatly strengthens the structural systematics within the lanthanide series, while also revealing very much stronger structural links with the actinide elements. Electronic structure calculations using the correct structure for the collapsed phases of Tb, Dy and Gd provide new insight into the behaviour of the $4f$ electrons at high density, and provide an explanation for the unusual magnetism seen in the collapsed phases of these elements.

II. EXPERIMENT

We focused our experimental study on the collapsed phase of Tb, which is obtained at a lower pressure (∼50 GPa) than in other lanthanides[26], thereby enabling the highest quality diffraction data to be collected, and which is reported to have an unusual magnetic state[12]. We conducted experiments on two separate Tb samples, reaching a maximum pressure of 110 GPa at 300 K. High-purity distilled samples were loaded into two diamond anvil cells in a dry argon atmosphere (<1 ppm O_2 and <1 ppm H_2O) to prevent oxidation. The first sample was loaded without a pressure medium but with a small piece of Ta foil as a pressure calibrant. The second sample was loaded in a He pressure medium without any pressure calibrant. Diffraction data were collected on the high-pressure ID09 beamline at the European Synchrotron Radiation Facility (ESRF) in Grenoble, (sample 1 and 2) and on the high-pressure I15 beamline at the Diamond Light Source (DLS) in the UK (sample 1). Monochromatic X-ray beams of wavelength $\lambda = 0.41177$ Å (ESRF) and 0.42454 Å (DLS), focused down to a FWHM of 10 μm (ESRF) and 20 μm (DLS), were used, and the powder diffraction data were recorded on MAR345 (DLS) and Mar555 (ESRF) area detectors, placed ∼350 mm from the sample. The sample pressure in sample 1 was derived from the published Ta equation of state[27], while the pressure in the sample 2 was determined from the Tb equation of state established using sample 1. The data used to solve the structure were obtained from sample 2. The 2D diffraction images were integrated using Fit2D[28], and the resulting 1D profiles were analysed using Rietveld and Le Bail fitting techniques[29], as well as least-squares fitting to the positions of individual diffraction peaks.

III. EXPERIMENTAL RESULTS

On compression, the onset of the transition to the collapsed phase was seen at 54(1) GPa, and single-phase diffraction patterns from it were seen above 64 GPa. The diffraction pattern from Tb at 64 GPa is shown in Figure

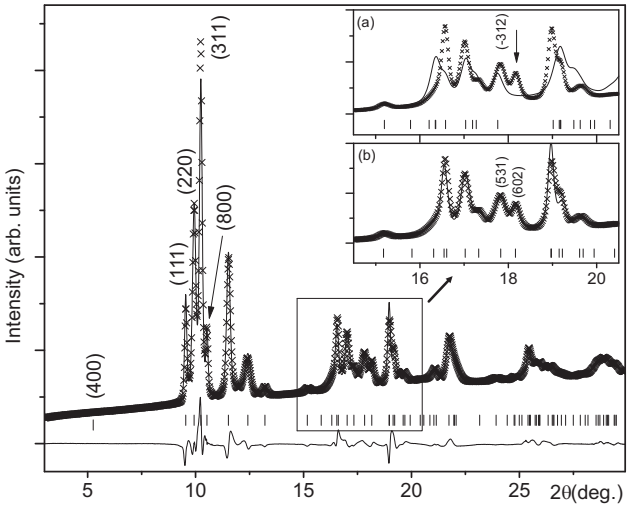

FIG. 2: Rietveld refinement of the $oF16$ structure to the Tb diffraction data at 64 GPa, showing the observed (crosses) and calculated (line) diffraction patterns, the calculated reflection positions (vertical lines), principal Miller indices, and difference profile (lower line). Space group $Fddd$, Tb on 16e (x,0,0) sites with x=3/16 (fixed), a=17.950(2) Å, b=4.933(1) Å, c=2.899(1) Å. The insets show Rietveld fits to the mid-angle region of the profile using (a) the $oC4$ structure and (b) the $oF16$ structures. The fit in (a) is clearly very poor, and amongst other misfits, the $mC4$ structure cannot account for the clear doublet at 18°. The fit provided by the $oF16$ is much better, and the doublet arises from the (531) and (602) peaks.

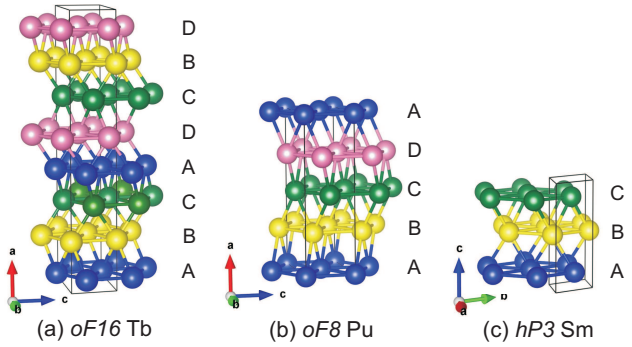

FIG. 3: The $oF16$ structure of Tb at 64 GPa, the $oF8$ structure of Pu at ambient pressure, and the $hP3$ structure of Sm at 47 GPa, all shown on the same scale. The structures each comprise stackings of quasi-close-packed hexagonal planes but with different stacking sequences. In all three structures the atoms within each layer are stacked over the saddle point of two atoms in the preceding layer, resulting in 10-fold coordination. This differs from the stacking of the layers of hcp and fcc etc, where the atoms are stacked over the midpoint of three atoms in the previous layer and the resulting coordination is 12-fold.

2, with inset (a) showing a Rietveld fit of the reported $mC4$ structure to the mid-angle region of this profile. This structure completely fails to fit the pattern above 2θ =16° (see Figure S1 for the $mC4$ fit to the full profile). In particular, there is a clear doublet at 2θ =18°, the higher-angle peak of which cannot be unaccounted for by the $mC4$ structure. The same doublet is evident in the published diffraction patterns from the collapsed phases of Dy, Ho, Er, and probably Tm (as detailed in the Supplementary Material[25]), while the diffraction data we have collected from the collapsed phase of Gd also exhibits the same doublet (Figure S2). The presence of this doublet shows that *none* of collapsed phases of Gd to Tm have the long-reported $mC4$ structure.

Ab initio indexing of the Tb data obtained at 64 GPa showed that all of the peaks could be accounted for by an orthorhombic unit cell with a=17.950(2) Å, b=4.933(1) Å, c=2.899(1) Å. The same cell fitted data collected to 110 GPa. The observed peaks and density uniquely identified the spacegroup as $Fddd$ with 16 atoms/cell. Placing the atoms on the 16e site at (x,0,0) gave an excellent fit, with x refining freely to 0.1874(4). The resulting structure comprises 8 layers of quasi-close-packed atoms stacked along the a-axis. If x=3/16=0.1875, then these layers are evenly spaced at x=1/16, 3/16 etc, and the intensity of the low-angle (400) peak at ∼5° (see Figure 2) is exactly zero. Lengthy X-ray exposures revealed no evidence of the (400) peak at any pressure, and so we have fixed x=3/16. The final Rietveld refinement with the $oF16$ structure is shown in Figure 2.

This $oF16$ unit cell is closely related to that of the previously reported $mC4$ cell, which is pseudo-orthorhombic[25], and fits all observed peaks, including the problematic doublet, with high precision (see inset (b) to Figure 2). The $oF16$ structure also fits our own data from the collapsed phase of Gd[25] and it also explains the doublets visible in the reported diffraction patterns from Gd, Ho, Er and (probably) Tm[25]. The collapsed phases of Gd-Tm therefore all have the $oF16$ structure.

The $oF16$ structure of Tb comprises 8 quasi-close-packed layers (b/c ∼sqrt(2.9)∼ $\sqrt{3}$) stacked along the a axis (see Figure 3a). Rather than the stacking seen in fcc, hcp, dhcp etc, where atoms in the close-packed layers are located above the midpoint between three atoms in the previous layer, in the $oF16$ structure the atoms are located above the saddle point between two atoms in the previous layer. This results in 10-fold (6+2+2) coordination, and the possibility of each layer to choose between three different positions relative to the previous layer. As a result, the $oF16$ structure of Tb has an 8-layer ABCADCBD repeat. Exactly the same type of layer stacking is seen in the iso-symmetric $oF8$ structure of Pu (which is also seen in Am, Cm and Cf on compression[8–10]), although this structure has only a 4-layer ABCD repeat (Figure 3b).

It is possible to predict other members of the same structural family, such as structures having 3-layer (ABC) or 6-layer (ABCADC) stacking sequences. Analysis of the $hP3$ structure reported in Nd, Sm and Yb shows

that this is the 3-layer ABC structure (Figure 3c)[30]. We note that the $hP3$ phase of Nd has recently been reported to exhibit the same rapid increase in magnetic ordering temperature seen in the $oF16$ phases of Tb and Dy[31], while the ordering temperature in $hP3$-Sm is relatively unchanged with pressure[32].

Furthermore, the monoclinic phase of Cm-III (space-group C2/c), which is stabilised by spin polarization of its $5f$ electrons, has a very similar structural motif to $hP3$[9], while the structure of Sc found above 240 GPa is only slightly distorted from $hP3$[33]. The collapsed phases of the regular trivalent lanthanides, divalent Yb, Pu at ambient pressure and high temperature, Am, Cm and Cf on compression, and Sc at extreme pressures are thus all members of this new family of elemental structures. The 6-layer ABCADC structure, and other possible members, remain to be identified.

The $oF16$ structure has not been reported previously in the elements, but was predicted to be a high-pressure form of Y, with the $oF16$ and $hP3$ phases being energetically favourable at pressures over 97 GPa[34]. While the similarity in the enthalpies of these two structures is perhaps not surprising given the structural similarities revealed here, the same calculations showed that the $oF8$ form of Y would have a somewhat higher enthalpy, and was unlikely to be observed. We note that the experimentally determined structure of collapsed Y above 100 GPa is the same $mC4$ structure of collapsed Tb etc[35]. New data are required to determine whether this phase too has the $oF16$ structure, which would further strengthen the structural systematics of Y and Sc with those of the lanthanides and actinides.

Finally, we address the structures of the collapsed $mC4$ phases of Nd and Sm which are obtained via a transition from the lower-pressure $hP3$ phase (Figure 1). The diffraction patterns of $mC4$-Nd[36] and $mC4$-Sm[37] are both very different to each other, and to those reported in the higher-Z lanthanides. The lattice parameters of $mC4$-Nd and Sm are also very different (β =118.6° in Nd at 89 GPa[36], and β =112.8° in Sm at 109 GPa[37]). However, the published diffraction pattern from $mC4$-Nd is strikingly similar to that reported for $oF8$-Am[8], and there is a clear relationship between the $mC4$ and $oF8$ unit cells[25]. As a result, Nd at 89 GPa can be fitted with the $oF8$ structure of γ-Pu with a =2.7160(1) Å b =4.8473(2) Å and c =8.8618(2) Å[25]. The $P6_222$ and $Fddd$ space groups of $hP3$-Nd and $oF8$-Nd are not group-subgroup related, but the previous determination of the equation of state of Nd to 155 GPa[22] revealed that there is no volume discontinuity at the $hP3 \rightarrow oF8$ transition, a result which, due to the close similarities of the lattices of the $mC4$ and $oF8$ structures[25], is unaffected by whether the higher-pressure phase is indexed as orthorhombic or monoclinic.

This first observation of the $oF8$ structure in a lanthanide element further strengthens the structural similarities of the lanthanide and actinide series, and reveals that the 3-, 4- and 8-layer structure types are all observed in the lanthanide elements. Further studies will be required to determine the true structure of the post-$hP3$ phase of Sm, which has recently been shown to exhibit the rapid increase in magnetic ordering temperature seen in the $oF16$ phases of Tb and Dy[32].

IV. ELECTRONIC STRUCTURE CALCULATIONS

Chen *et al.*'s calculations on Y showed that the shift of the d electron energy levels and s-to-d electron transfer gave rise to the stability of the $oF16$ and $hP3$ structures. As Y has no f electrons, their role in stabilising the $oF16$ structure in the lanthanides was undetermined. To address this, we have performed extensive DFT and DMFT calculations of the $oF16$ phases of Tb, Gd and Dy.

Structural optimization of bulk Tb in the $mC4$ and $oF16$ phases was accomplished by using spin-polarised DFT calculations with the help of the VASP[38] package using the PBE functional[39]. The many-body properties of the $mC4$ and $oF16$ phases were further investigated by using a recent implementation of DFT+Dynamical Mean-Field Theory (DFT+DMFT) in the CASTEP code[40–42]. The k-point sampling was done using a Monkhorst-Pack mesh of 8×8×8 for the $oF16$ and 10×10×6 for the $mC4$ structures, respectively, and a Gaussian smearing of 0.1 eV. Convergence in DFT over k-points was achieved within 1 meV per atom, and the energy cutoff was 800 eV. Scalar relativistic spin-orbit coupling was taken into account within the Koelling-Harmon approximation[43].

In the DMFT, we used the Hubbard I solver, valid for f-elements. In this manuscript, we focused on the DMFT approach within the framework of fixed Kohn-Sham (KS) potentials, the so-called "one-shot" DFT+DMFT method. This has been shown to predict the equilibrium volume and bulk modulus for f materials that are in excellent agreement with experimental data[40]. We use typical values for the Coulomb repulsion (U = 6 eV) and Hund's coupling (J = 1 eV). Throughout this paper we performed DFT+DMFT calculations with fixed charge and used the Fully Localised Limit (FLL) type of double counting corrections.

Zero temperature DFT calculations for Tb confirmed that the $oF16$ phase is stable with respect to $mC4$ above 60 GPa (see Figure 3), and the predicted atomic volume of the $oF16$ phase is in good agreement with the room temperature experimental data. Calculations of the phonon spectrum of $oF16$-Tb at 80 GPa (see Figure S6) structure verified its stability (no soft phonons). We see no evidence of the $mC4$ phase at any pressure in our (room temperature) diffraction studies. The ground states of both the $mC4$ and $oF16$ phases are calculated to be ferromagnetic, but in the $oF16$ phase between 60 and 80 GPa the energy difference between the ferromagnetic (F) and anti-ferromagnetic (AF) state is of the order of room temperature, suggesting that competition

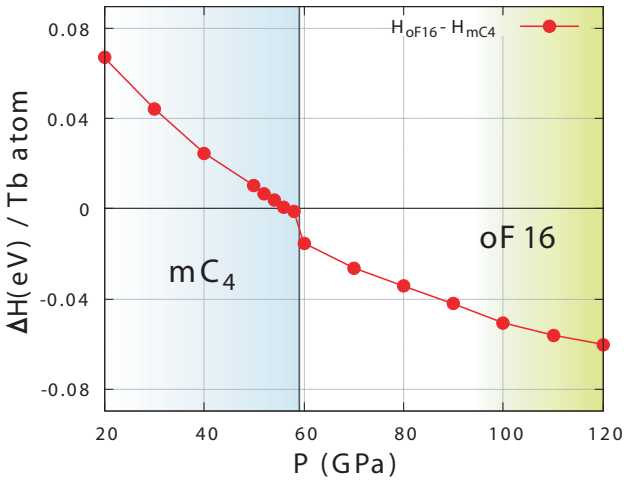

FIG. 4: The enthalpy difference per Tb atom as a function of pressure as predicted by magnetic DFT. The calculations were performed at 0 K.

between these different magnetic states might occur in this pressure range. This may account for the highly non-monotonic behaviour of the magnetic ordering temperature observed in Tb near 70 GPa by Lim *et al.*[44]. Remarkably, the AF phase in Tb is stabilized via a gain of internal electronic energy, but at the cost of a lattice expansion. This rules out the possibility for AF order at higher pressures. In Gd however (see discussion below), the AF order is concomitant with a reduction of the volume, and hence is naturally stabilized at higher pressures.

We emphasize that the remarkable agreement between theory and experiments can only be achieved within spin-polarised DFT which accounts for the strong magnetic moments due to f electrons: the simpler non-magnetic DFT approach does not provide a reasonable equation of state, confirming the importance of magnetism for the structural properties above 60 GPa. Indeed, the volume obtained at 60 GPa in non-magnetic calculations is 14% lower than the experimental value, whereas magnetic calculations calculate the atomic volume to within 1.5% of the experimental value.

While the magnetism in Tb is not stable at room temperature, at which our experiments have been carried out, a local fluctuating magnetic moment due to f states is expected to persist in the paramagnetic state at 300 K. It is therefore important to properly describe the dynamical fluctuations of local magnetic moments within the theoretical framework, which is not achievable within DFT calculations and requires extensions.

For this, we carried out DFT+DMFT calculations at room temperature. Figure 5 shows the calculated spectral weight in the paramagnetic DFT+DMFT solution. Although the DMFT approximation does not have long-range magnetic order, it describes the fluctuations of the local magnetic moment of the Tb atoms. Note that in

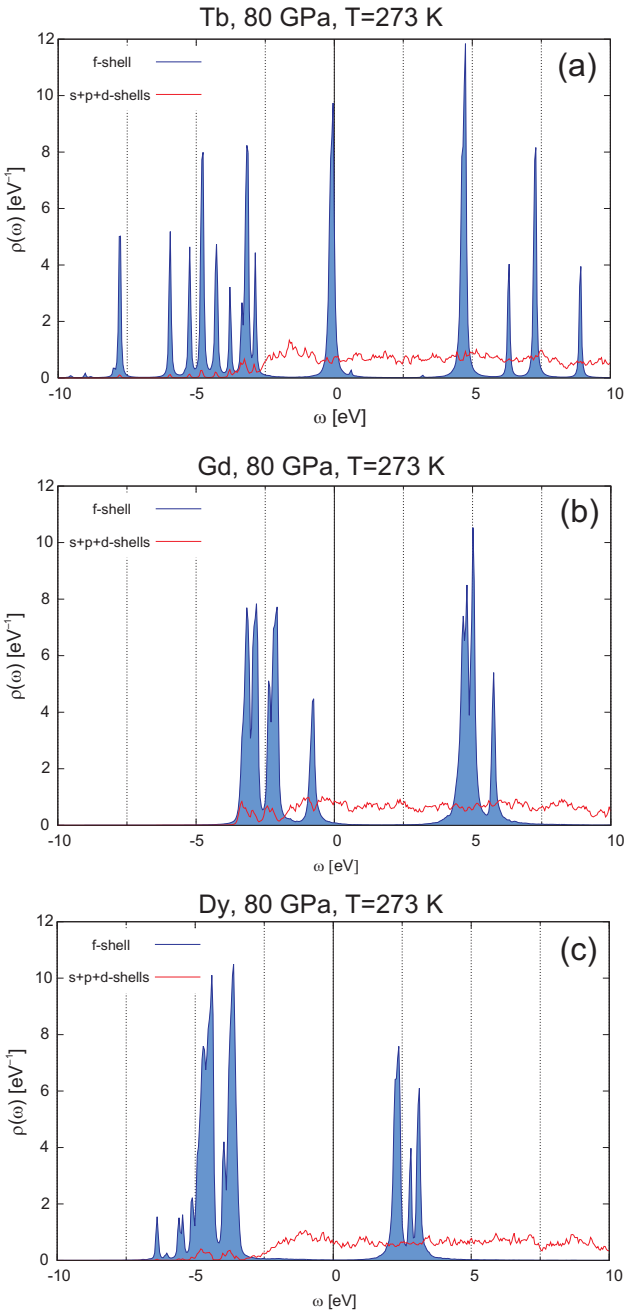

FIG. 5: Spectral weight $\rho(\omega)$ obtained at room temperature and 80 GPa for the $oF16$ phases a) Tb , b) Gd, and c) Dy. The sum of the s, p and d orbitals are shown in red and the f in blue.

DMFT we observe sharp resonances corresponding to the splitting of the f states into magnetic multiplets (see Figure 5a), with the majority spin states at -5 eV and the minority spin states at $+7$ eV.

Additionally, we also obtain a sharp peak at the Fermi level (at $\omega = 0$, see Figure 5a). This narrow feature is absent at simpler levels of approximations (such as DFT), and although it does not impact on averaged quantities,

such as forces or magnetism, it sheds light on possible emerging excitations, important for thermo-mechanical constants and specific heat coefficients.

The picture of the collapsed phase of Tb that emerges from our calculations is that of a lattice of unscreened weakly-coupled local moments embedded in a delocalised d-conduction band with a large band width. As discussed in the DFT context, the unscreened moments are key for the correct description of the structure at high pressure. On compression (see Figure S5), we observe only minor changes of the overall spectral weight, and the magnetic moment remains a sextet $S = \frac{5}{2}$ at all pressures studied.

Our finding that the collapsed phases of Dy and Gd also have the $oF16$ structure prompted us to expand our DFT calculations to these two elements, which are reported to exhibit different magnetic behaviours under pressure[44]. At 90 GPa and 0 K, our calculations confirm the $oF16$ phase to energetically favourable compared to the $mC4$ phase in both Dy and Gd – although in Gd the $mC4$ phase is calculated to be more stable below 90 GPa. Our room temperature diffraction studies of Gd see no evidence of the $mC4$ phase at any pressure.

At 90 GPa and 0 K $oF16$-Gd is calculated to be a type-A antiferromagnet, while $oF16$-Dy is calculated to be a ferromagnet. This contrasts with the results for Tb which identify it as a Kondo ferromagnet, nearly degenerate with an anti-ferromagnetic state between 60 GPa and 80 GPa. Our calculations show that the magnetic order in Dy is much more robust than in Tb and Gd, in agreement with the higher magnetic ordering temperature observed by Lim *et al.*[44]. Indeed, the enthalpy difference in Dy between the ferro and anti-ferromagnetic states is 0.14 eV/atom, while in Tb and Gd it is $\approx |0.06|$ eV/atom at 110 GPa.

For all three elements, the spin magnetic moment of the f-shell persists at room temperature at 80 GPa – $S = 3\mu_B$ in Gd, $S = 2.5\mu_B$ in Tb and $S = 2\mu_B$ in Dy, although the long range magnetic order is lost. These magnetic moments are approximately $0.5\mu_B$ smaller as compared to the respective free ions due to the transfer of approximately one electron from the f-shell to the d-shell as a consequence of applied pressure. However, the different magnetic behaviour of the materials can be inferred by their different paramagnetic properties. In particular, as anti-ferromagnetism is stablized by RKKY processes[45,46] mediated by conduction electrons, the hybridisation between f and d states is key to obtaining antiferromagnetic order. Our calculations reveal that the f and d states are indeed hybridised in Gd (see Figure 5b), whereas such hybridisation is absent in Dy (see Figure 5c). Indeed, in Dy the f states are below the Fermi level (between -7 eV and -3 eV) and are very weakly hybridised to the d-states, as the weight of these states is weak in this energy window (see red curve in Figure 5c between -7 eV and -3 eV).

V. CONCLUSIONS

The assignment of the $oF16$ structure to the collapsed phases of Tb, Gd, Dy, Ho, Er and Tm rewrites the long-established structural systematics of the lanthanide elements, while the $oF16$ structure's close similarity to the isosymmetric $oF8$ structure seen in Pu, Am, Cf and Cm reveals a previously-unrecognised relationship between the high-pressure phases of the lanthanide and actinides series. This is reinforced further by the discovery that the highest-pressure phase of Nd also has the same $oF8$ structure, and that the $oF16$ and $oF8$ structures, and the $hP3$ structure found in Nd, Sm and Yb, are all members of a new family of elemental crystal structures. Further members of this family are predicted and remain to be discovered.

State-of-the-art quantum many-body calculations using the correct structure for the collapsed phase provide new insights into the physics of f elements at high pressure, and in particular highlight that Kondo-type physics, and more generally magnetism, can be sustained at extreme pressure, a question that has long eluded scientists of the field, as emergent quantum phenomena such as Kondo are associated with exponentially small energy scales. The joint experimental and theoretical approach confirms that magnetism of the $4f$ electrons is correctly accounted for, and a classification of typical lanthanides has been obtained in terms of ferro-magnetism, anti-ferromagnetism, and Kondo for respectively Dy, Gd and Tb. The interplay between structural properties and electronic properties accounts for the stability of anti-ferromagnetism in Gd, absent in Tb.

VI. ACKNOWLEDGMENTS

 This work was supported by grants (EP/R02927X/1 and EP/R02992X/1) from the UK Engineering and Physical Sciences Research Council (EPSRC), and facilities made available by the European Synchrotron Radiation Facility and Diamond Light Source. We thank U. Schwarz for providing the Tb and Gd samples, and D. Daisenberger and A. Kleppe for their support on the beam lines. M.I.M. is grateful to AWE for the award of a William Penney Fellowship. The computational work was supported by the ARCHER UK National Supercomputing Service and the UK Materials and Molecular Modeling Hub for computational resources (EPSRC Grant No. EP/P020194/1

[1] U. Benedict, W. A. Grosshans, and W. B. Holzapfel, Physica B & C **144**, 14 (1986).

[2] W. B. Holzapfel, Physica B: Condensed Mat-

ter **190**, 21 (1993), ISSN 0921-4526, URL http://www.sciencedirect.com/science/article/pii/092145269390438C.

[3] W. B. Holzapfel, Journal of Alloys and Compounds **223**, 170 (1995), ISSN 0925-8388, URL http://www.sciencedirect.com/science/article/pii/0925838894090017.

[4] K. Gschneidner, Journal of Alloys and Compounds **223**, 165 (1995), ISSN 0925-8388, URL http://www.sciencedirect.com/science/article/pii/0925838894090009.

[5] B. Johansson, Hyperfine Interactions **128**, 41 (2000), ISSN 1572-9540.

[6] G. K. Samudrala and Y. K. Vohra, in *Including Actinides*, edited by J.-C. G. Bnzli and V. K. Pecharsky (Elsevier, 2013), vol. 43 of *Handbook on the Physics and Chemistry of Rare Earths*, pp. 275 – 319, URL http://www.sciencedirect.com/science/article/pii/B9780444595362000040.

[7] F. PORSCH and W. B. HOLZAPFEL, Physical Review B **50**, 16212 (1994).

[8] S. Heathman, R. G. Haire, T. Le Bihan, A. Lindbaum, K. Litfin, Y. Méresse, and H. Libotte, Phys. Rev. Lett. **85**, 2961 (2000), URL https://link.aps.org/doi/10.1103/PhysRevLett.85.2961.

[9] S. Heathman, R. G. Haire, T. Le Bihan, A. Lindbaum, M. Idiri, P. Normile, S. Li, R. Ahuja, B. Johansson, and G. H. Lander, Science **309**, 110 (2005), ISSN 0036-8075, http://science.sciencemag.org/content/309/5731/110.full.pdf, URL http://science.sciencemag.org/content/309/5731/110.

[10] S. Heathman, T. Le Bihan, S. Yagoubi, B. Johansson, and R. Ahuja, Phys. Rev. B **87**, 214111 (2013), URL https://link.aps.org/doi/10.1103/PhysRevB.87.214111.

[11] G. Fabbris, T. Matsuoka, J. Lim, J. R. L. Mardegan, K. Shimizu, D. Haskel, and J. S. Schilling, Phys. Rev. B **88**, 245103 (2013), URL https://link.aps.org/doi/10.1103/PhysRevB.88.245103.

[12] J. Lim, G. Fabbris, D. Haskel, and J. S. Schilling, Phys. Rev. B **91**, 174428 (2015), URL https://link.aps.org/doi/10.1103/PhysRevB.91.174428.

[13] J. Lim, G. Fabbris, D. Haskel, and J. S. Schilling, Phys. Rev. B **91**, 045116 (2015), URL https://link.aps.org/doi/10.1103/PhysRevB.91.045116.

[14] R. J. Husband, I. Loa, G. W. Stinton, S. R. Evans, G. J. Ackland, and M. I. McMahon, Phys. Rev. Lett. **109**, 095503 (2012), URL http://link.aps.org/doi/10.1103/PhysRevLett.109.095503.

[15] R. J. Husband, I. Loa, K. A. Munro, E. E. McBride, S. R. Evans, H.-P. Liermann, and M. I. McMahon, Phys. Rev. B **90**, 214105 (2014), URL https://link.aps.org/doi/10.1103/PhysRevB.90.214105.

[16] W. H. Zachariasen, Proceedings of the National Academy of Sciences of the United States of America **75**, 1066 (1978), ISSN 1091-6490, URL http://www.ncbi.nlm.nih.gov/pmc/articles/PMC411408/.

[17] Y. C. Zhao, F. Porsch, and W. B. Holzapfel, Phys. Rev. B **50**, 6603 (1994), URL https://link.aps.org/doi/10.1103/PhysRevB.50.6603.

[18] R. J. Husband, I. Loa, K. Munro, and M. I. McMahon, Journal of Physics: Conference Series **500**, 032009 (2014), URL https://doi.org/10.1088%2F1742-6596%2F500%2F3%2F032009.

[19] G. N. Chesnut and Y. K. Vohra, Phys. Rev. Lett. **82**, 1712 (1999), URL https://link.aps.org/doi/10.1103/PhysRevLett.82.1712.

[20] F. H. Ellinger and W. H. Zachariasen, Phys. Rev. Lett. **32**, 773 (1974), URL https://link.aps.org/doi/10.1103/PhysRevLett.32.773.

[21] G. S. Smith and J. Akella, Journal of Applied Physics **53**, 9212 (1982), https://doi.org/10.1063/1.330393, URL https://doi.org/10.1063/1.330393.

[22] G. N. Chesnut and Y. K. Vohra, Phys. Rev. B **61**, R3768 (2000), URL https://link.aps.org/doi/10.1103/PhysRevB.61.R3768.

[23] S. Endo, H. Sasaki, and T. Mitsui, Journal of the Physical Society of Japan **42**, 882 (1977), https://doi.org/10.1143/JPSJ.42.882, URL https://doi.org/10.1143/JPSJ.42.882.

[24] Y. K. Vohra and J. Akella, High Pressure Research **10**, 681 (1992), https://doi.org/10.1080/08957959208225319, URL https://doi.org/10.1080/08957959208225319.

[25] See Supplemental Material (LINK) for additional information on the issues with the previous X-ray data, and discussions of the relationship between the $oF16$, $oF8$ and $mC4$ structures, which includes Refs.[47–53].

[26] N. C. Cunningham, W. Qiu, K. M. Hope, H.-P. Liermann, and Y. K. Vohra, Phys. Rev. B **76**, 212101 (2007), URL https://link.aps.org/doi/10.1103/PhysRevB.76.212101.

[27] T. S. Sokolova, P. I. Dorogokupets, A. M. Dymshits, B. S. Danilov, and K. D. Litasov, Computers & Geosciences **94**, 162 (2016), ISSN 0098-3004.

[28] A. P. Hammersley, S. O. Svensson, M. Hanfland, A. N. Fitch, and D. Hausermann, High Press Res. **14**, 235 (1996).

[29] V. Petricek, M. Dusek, and L. Palatinus, Zeitschrift fur Kristallographie - Crystalline Materials **229**, 345 (2014), ISSN 21967105.

[30] The spacegroup of the $hP3$ phase of Sm was originally reported as $P3_121$, with atoms on the $3a$ site at $(x,0,\frac{1}{3})$ with x=0.45 and c/a =2.36[17]. To date, the $hP3$ structure has been regarded as a distortion of fcc, and the two would be equivalent if $x = \frac{1}{3}$ and c/a =2.45[17]. More recently, however, using Rietveld refinement, Husband *et al* reported that x =0.513(5)[18]. Chen *et al* have noted that if $x = \frac{1}{2}$, then the symmetry of the $hP3$ structure becomes $P6_222$[34]. As this structure has different systematic absences to $P3_121$, these can be used to distinguish the two stuctures. Reanalysis of the data reported in Husband *et al*[18] reveals that the absences are indeed consistent with spacegroup $P6_222$ rather than $P3_121$, and hence $x = \frac{1}{2}$.

[31] J. Song, W. Bi, D. Haskel, and J. S. Schilling, Phys. Rev. B **95**, 205138 (2017), URL https://link.aps.org/doi/10.1103/PhysRevB.95.205138.

[32] Y. Deng and J. S. Schilling, Phys. Rev. B **99**, 085137 (2019), URL https://link.aps.org/doi/10.1103/PhysRevB.99.085137.

[33] Y. Akahama, H. Fujihisa, and H. Kawamura, Physical Review Letters **94**, 195503 (2005), ISSN 0031-9007.

[34] Y. Chen, Q.-M. Hu, and R. Yang, Phys. Rev. Lett. **109**, 157004 (2012), URL https://link.aps.org/doi/10.1103/PhysRevLett.109.157004.

[35] G. K. Samudrala, G. M. Tsoi, and Y. K. Vohra, Journal of Physics: Condensed Matter **24**, 362201 (2012), URL http://stacks.iop.org/0953-8984/24/i=36/a=362201.

[36] J. Akella, S. T. Weir, Y. K. Vohra, H. Prokop, S. A. Catledge, and G. N. Chesnut, Journal of Physics-

Condensed Matter **11**, 6515 (1999).
[37] G. N. Chesnut, Ph.D. thesis, The University of Alabama at Birmingham (2001).
[38] G. Kresse and D. Joubert, Phys. Rev. B **59**, 1758 (1999).
[39] J. P. Perdew, K. Burke, and M. Ernzerhof, Phys. Rev. Lett. **77**, 3865 (1996).
[40] E. Plekhanov, P. Hasnip, V. Sacksteder, M. Probert, S. J. Clark, K. Refson, and C. Weber, Phys. Rev. B **98**, 075129 (2018).
[41] M. C. Payne, M. P. Teter, D. C. Allan, T. A. Arias, and J. D. Joannopoulos, Rev. Mod. Phys. **64**, 1045 (1992).
[42] S. J. Clark, M. D. Segall, C. J. Pickard, P. J. Hasnip, M. I. J. Probert, K. Refson, and M. C. Payne, Zeitschrift fur Kristallographie - Crystalline Materials **220**, 567 (2005), ISSN 21967105.
[43] D. D. Koelling and B. N. Harmon, Journal of Physics C: Solid State Physics **10**, 3107 (1977), URL `https://doi.org/10.1088%2F0022-3719%2F10%2F16%2F019`.
[44] J. Lim, G. Fabbris, D. Haskel, and J. S. Schilling, Journal of Physics: Conference Series **950**, 042025 (2017), URL `http://stacks.iop.org/1742-6596/950/i=4/a=042025`.
[45] M. Petersen, J. Hafner, and M. Marsman, Journal of Physics: Condensed Matter **18**, 7021 (2006).
[46] L. W. Roeland, G. J. Cock, F. A. Muller, A. C. Moleman, K. A. McEwen, R. G. Jordan, and D. W. Jones, Journal of Physics F: Metal Physics **5**, L233 (1975).
[47] G. K. Samudrala and Y. K. Vohra, Journal of Physics: Conference Series **377**, 012111 (2012).
[48] Y. K. Vohra, B. R. Sangala, A. K. Stemshorn, and K. M. Hope, MRS Proceedings **1104**, 1104NN01 (2008).
[49] G. K. Samudrala, S. A. Thomas, J. M. Montgomery, and Y. K. Vohra, Journal of Physics: Condensed Matter **23**, 315701 (2011).
[50] J. M. Montgomery, G. K. Samudrala, G. M. Tsoi, and Y. K. Vohra, Journal of Physics: Condensed Matter **23**, 155701 (2011).
[51] D. Errandonea, R. Boehler, B. Schwager, and M. Mezouar, Phys. Rev. B **75**, 014103 (2007).
[52] G. K. Samudrala, G. M. Tsoi, S. T. Weir, and Y. K. Vohra, High Pressure Research **34**, 385 (2014), https://doi.org/10.1080/08957959.2014.977277.
[53] A. Togo and I. Tanaka, Scripta Materialia **108**, 1 (2015), ISSN 1359-6462, URL `http://www.sciencedirect.com/science/article/pii/S1359646215003127`.